Investigation of Continuous-jet Nozzle Design and Fabrication for Three Dimensional Printing

by

Tiina Hämeenanttila

Submitted to the Department of Mechanical Engineering
in Partial Fulfillment of the Requirements for the Degree of

Bachelor of Science in Mechanical Engineering

at the
Massachusetts Institute of Technology
May 1994

© Massachusetts Institute of Technology, 1994
All rights reserved

Signature of Author _____
Department of Mechanical Engineering
May 6, 1994

Certified by _____
Professor Emanuel M. Sachs
Associate Professor of Mechanical Engineering
Thesis Supervisor

Accepted by _____
Professor Peter Griffith
Chairman, Department Committee

ARCHIVES

MASSACHUSETTS INSTITUTE
OF TECHNOLOGY

JUL 13 1994

LIBRARIES

Investigation of Continuous-jet Nozzle Design and Fabrication for Three Dimensional Printing

by

Tiina Hämeenanttila

Submitted to the Department of Mechanical Engineering
on May 6, 1994 in partial fulfillment of the requirements for
the degree of Bachelor of Science

Abstract

This report describes the design, fabrication, and characteristics of a rubber orifice, piezo-electric, continuous-jet nozzle suitable for Three Dimensional Printing. Future innovations in Three Dimensional Printing will demand nozzles with robust operating characteristics over a wide range of driving frequencies and fluid flow rates.

Three Dimensional Printing is a rapid prototyping process which creates functional prototypes or tooling for industry directly from CAD models. The parts are formed by successively printing cross-sectional layers of the final 3D shape, so complex geometries and under cuts can be achieved. The process involves continuous-jet printing technology, which uses piezo-electric vibration to break up a stream of fluid into a regular and controllable train of droplets which are then printed onto a bed of alumina or stainless-steel powder or deflected away into a catcher. In order to print with a wide range of fluids, flow rates, and driving frequencies, new nozzles are constantly being sought.

From several design ideas, a nozzle which has a rubber orifice molded inside a radially polarized piezo-electric ceramic tube emerged with characteristics suitable for Three Dimensional Printing. A rubber orifice was fabricated with an exit diameter comparable to the ones traditionally used on the 3D Printing machine, of approximately 50μm, and the desired range of flow rates, piezo driving frequency, and stream breakoff length were achieved while testing with water.

Thesis Supervisor: Emanuel Sachs
Title: Associate Professor of Mechanical Engineering

Acknowledgments

I would like to acknowledge the support of the NSF Strategic Manufacturing Initiative, MIT Leaders for Manufacturing, ARPA, 3DP Medical/J&J and the members of the 3D printing consortium- Ashland Chemical, Draper Laboratories, Howmet, Johnson & Johnson, Boeing, AMP, Hasbro, 3M, Proctor & Gamble, Sandia National Laboratories, and United Technologies.

I would also like to thank Ely Sachs for supporting my work on a challenging and rewarding thesis.

Jim Serdy, whose ideas, know-how, and inspirations were often the driving influence behind nozzle design, fabrication, and testing.

and

Jim Bredt for sharing his knowledge of materials, lab practice, and common pit-falls.

Table of Contents

List of Figures

Chapter 1 -- Introduction

1.1 - Three Dimensional Printing

Three Dimensional Printing is an innovative rapid-prototyping process capable of reducing the lead time of protoytpe parts or machine tooling from weeks to days. Currently, prototype and tooling fabrication involve many labor-intensive, slow, and costly steps, which 3D Printing proposes to do in one step. The time and cost savings afforded by 3D Printing will revolutionize prototyping and manufacturing processes once 3D Printing is fully developed.

The 3D Printing process fabricates a part from a CAD model specified in three dimensions. A slicing algorithm divides the part into cross sectional layers, approximately 175μm thick, and creates detailed information about each cross-section. As illustrated in Figure 1, 3D Printing begins with a layer of spread powder. The 3D Printing machine then selectively prints a binder fluid onto a powder bed in the shape of the cross-section of the part, much like an ink-jet printer prints a picture on paper. The powder bed is then lowered, and a new layer of powder is spread. This process repeats until the entire part has been printed. After firing, the loose (unprinted) powder is removed. In addition to shortening lead time, 3D Printing can create complex geometries and under cuts which conventional manufacturing techniques cannot.

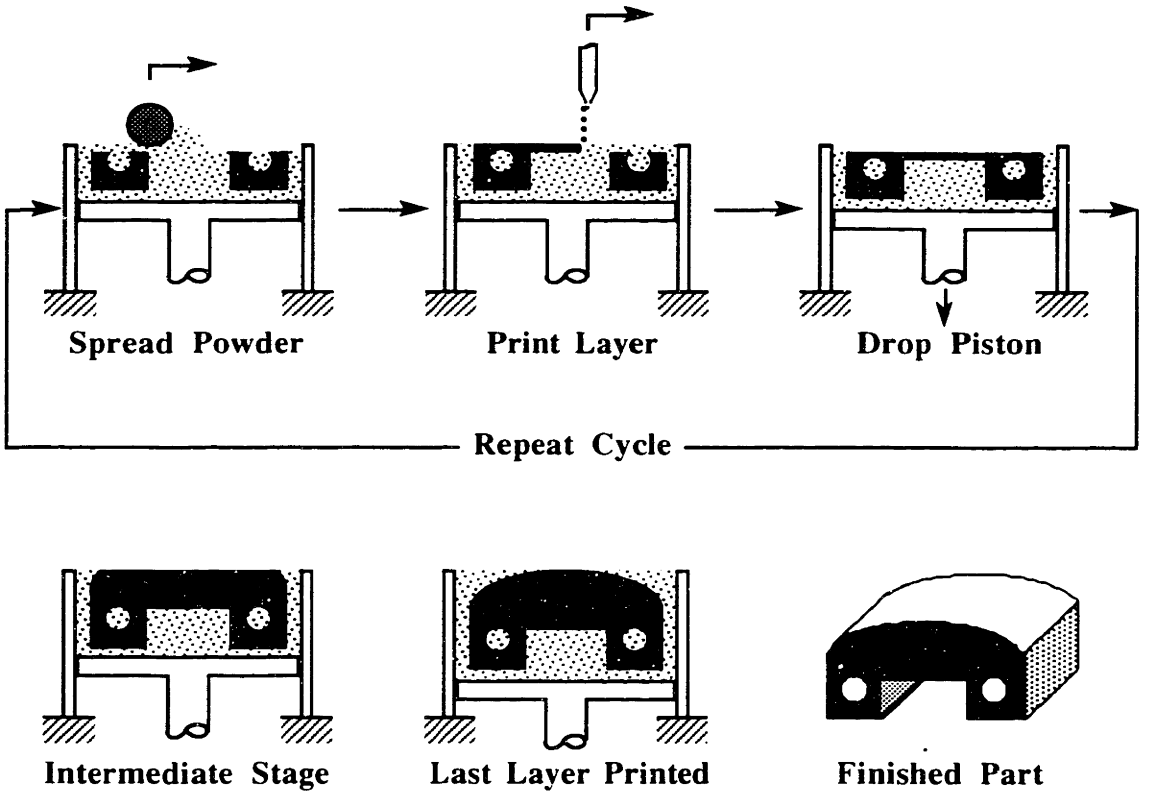

Figure 1 - The 3D Printing process

1.2 - Continuous-jet Nozzles

Continuous-jet printing in both ink-jet printers and 3D Printing relies on the breakup of a cylindrical stream into droplets. These droplets are then given an electrical charge by passing the stream at the point of droplet breakoff between two conductive parallel plates, where the stream becomes a conductor in a parallel-plate capacitor. The amount the charge that a droplet gains is proportional to the potential difference between the plates and the stream [Williams, p.55-56]. The direction of the droplets either onto the powder bed or into a separate fluid catcher can be decided by passing the droplets through an electric field formed by a second set of parallel plates. Charged droplets will deflect into

the catcher, uncharged droplets will print on the powder bed [ibid.]. For precise droplet control, the breakoff length of the stream and the frequency of droplet formation must be known and reliable.

A cylindrical stream is inherently unstable and bound to breakup into a train of spherical droplets because the surface area, and therefore surface energy, of a cylinder is greater than the surface area, and surface energy, of a string of spheres which total the same volume. Any disturbance of the cylindrical stream will therefore collapse the stream and cause droplet formation.

These disturbances grow exponentially on the surface of the stream until it breaks up. When the stream is disturbed with vibrational energy, certain vibrational frequencies will grow faster exponentially than others, and the droplets will break off from the cylindrical stream at the dominant frequency. This frequency is predicted for an inviscid fluid jet in a vacuum, with the assumption that the stream was subject to a wide spectrum of vibrational frequencies which all had the same amplitude. The characteristic (Rayleigh) frequency is calculated as [Williams, p.53]:

$$f = \frac{v}{4.51\ d} \tag{1}$$

where f is the frequency, v is the jet velocity and d is the jet diameter.

By assuming axisymmetrical disturbances and exponential disturbance growth, Rayleigh also estimated the distance the stream will travel before complete droplet breakoff occurs. For the inviscid case [ibid.]:

$$\frac{Z}{d} = 1.03 \left(\ln \frac{d}{2\delta_r} \right) \sqrt{We} \tag{2}$$

where Z is the break off length, δ_0 is the initial infinitesimal disturbance at the nozzle orifice measured as a change in diameter of a circular stream, and We is the fluid's Weber number, given by:

$$We = \frac{\rho v^2 d}{\gamma} \tag{3}$$

where ρ is the density of the fluid and γ is the fluid's surface tension.

To account for the effects of fluid viscosity, Weber calculated the distance before breakoff as [Williams, p.54]:

$$\frac{Z}{d} = \ln\frac{d}{2\delta_0}\left[\sqrt{We} + 3\frac{We}{Re}\right] \tag{4}$$

where Re is the fluid's Reynolds number, given by:

$$Re = \frac{\rho v d}{\mu} \tag{5}$$

where μ is the viscosity of the fluid. For water, the Reynolds number is seven times greater than the Weber number. For colloidal silica binder used in 3D Printing, the Reynolds number is slightly less than the Weber number. Therefore, according to equation 4, silica binder breaks up about 50% later for binder than for water [Williams, p.54].

For 3D Printing, typical values for printing are an orifice diameter of 50μm and a fluid flow rate in the range of 1.0 cc/min to 1.5 cc/min. These result in jet velocities from 10m/s to 15m/s and Rayleigh frequencies (approximated with the inviscid case) ranging from 45kHz to 65kHz. For use with 3D Printing, new nozzle designs should be within these ranges.

Chapter 2 -- Motivation for New Nozzle Designs

2.1 - Smaller and Lighter Nozzles

One of the next steps in upgrading the 3D Printing process will be to move from a single continuous-jet nozzle to multiple continuous-jet nozzles. Using smaller and lighter nozzles in a multiple jet application would be advantageous. Current progress involves replacing the single nozzle with a commercially available ink-jet nozzle from the suppliers Diconix, Imaje, or Domino. All of these nozzles use piezo motion to form a pressure wave which forces the fluid through the orifice at the piezo frequency. These nozzles are tuned to operate at mechanical resonance, either resonance of piezo stacks which act on the fluid just over the orifice in the case of the Imaje and Domino nozzles, or resonance of the entire fluid chamber which is expanded and compressed by piezo strips in the case of the Diconix nozzle. To get the mechanical resonance in the range of 60-80kHz, which creates suitable drop sizes and spacings, these nozzles are relatively massive to balance out other mechanical resonant effects. For example, the Domino nozzle, which has been selected as the multiple-jet nozzle upgrade for 3D Printing, weights 323g and is designed to operate from 60-64kHz. However, part of the weight comes from the use of stainless steel which is corrosion resistant but heavy, and since the nozzle is usually stationary in operation, size and weight were not critical factors in its design. Also, the piezo stacks are powerful enough to produce clean droplet breakoff far out of the prescribed operating range. But while these types of nozzles could be reduced in size and weight to better suit 3D Printing, the piezo stacks or strips and the fluid chamber would still be relatively large and rely on powerful operation to generate droplets.

While this multiple-jet nozzle technology is reliable, it does have disadvantages in flexibility. For one, the piezo excitation for each orifice comes from the same driving voltage in the commercially available nozzles, so that each stream necessarily has the same

frequency of droplet formation. Also, all of the jets must be tuned to the same frequency, and this frequency is fixed around the resonant operating frequency. All of the jets have to same the fluid source as well, so advances in printing with various binders on the same printing run would requires the entire nozzle or the entire fluid delivery to be changed. And for maintenance, if any one of the eight nozzles becomes clogged, the entire nozzle must be cleaned. Single nozzles which are small enough to be placed close together to form a multiple-jet printhead would have the advantages of individual frequency tuning, fluid type, and maintenance. The distance between jets on the new eight-jet nozzle is 4.2mm, so individual nozzles about 4-5mm in width could be lined up or arranged in a compact pattern to form a comparable multiple-jet nozzle.

Reducing the weight of the nozzles is also advantageous. During operation over a stationary powder bed, the nozzle begins at a dead stop, and is then accelerated to a constant speed of about 1.5m/s over the powder bed, and then decelerated to a stop and accelerated across the powder bed in the opposite direction. A lighter nozzle would need less force to bring it up to speed, or require a shorter ramp-up distance before traveling over the powder bed.

2.2 - More Efficient Transfer of Piezo Energy to the Fluid

One area of interest in new nozzle design is bringing the piezo motion directly to the surface of the fluid stream. From either of the breakoff length equations 2 or 4, it is clear that as the initial surface disturbance δ_0 increases, the breakoff length decreases. To a point, a shorter breakoff length is desirable because then the total length needed to generate droplets, charge the droplets and deflect the droplets is reduced. Therefore the total distance from the nozzle orifice to the powder bed is reduced. As the time of flight of the droplets decreases, the effects of air drag, air currents, and printhead motion decreases. On

the other hand, typical breakoff lengths are on the order of 1/20in, while the total distance from the nozzle orifice to the powder bed is about 1.3in, so large reductions in breakoff length will not have a large impact on the total distance of droplet travel. Also, droplet charging takes place during breakoff, and room to fit the charging cell is needed.

Increasing the strength of the piezo excitation energy may also eliminate satellite drops [Williams, p.55]. Satellite drops are extra, small droplets formed by imperfect stream breakoff. These satellite drops can merge with a larger droplet, changing the total charge and consequently the deflection of the droplet, or land on the powder bed or the catcher in an undesirable place. Efficient transfer of piezo energy directly to the fluid stream may result in nozzles which eliminate satellite drops as a natural part of their operation.

2.3 - Greater Operating Frequency Range

The nozzles currently used on the 3D Printing machine are tuned to operate at a single resonant frequency in order to take advantage of the increased amplitude response at resonance, thereby increasing the amount of excitation energy for stream breakoff and resulting in a short breakoff length and well formed droplets. However, if a nozzle could have an equal amplitude response over a range of frequencies, several advantages in operation could be gained. Modeling the nozzle as a second order system and studying a resonant Bode plot of amplitude vs. frequency as shown in figure 2, provides a good illustration of a potentially desirable nozzle frequency response.

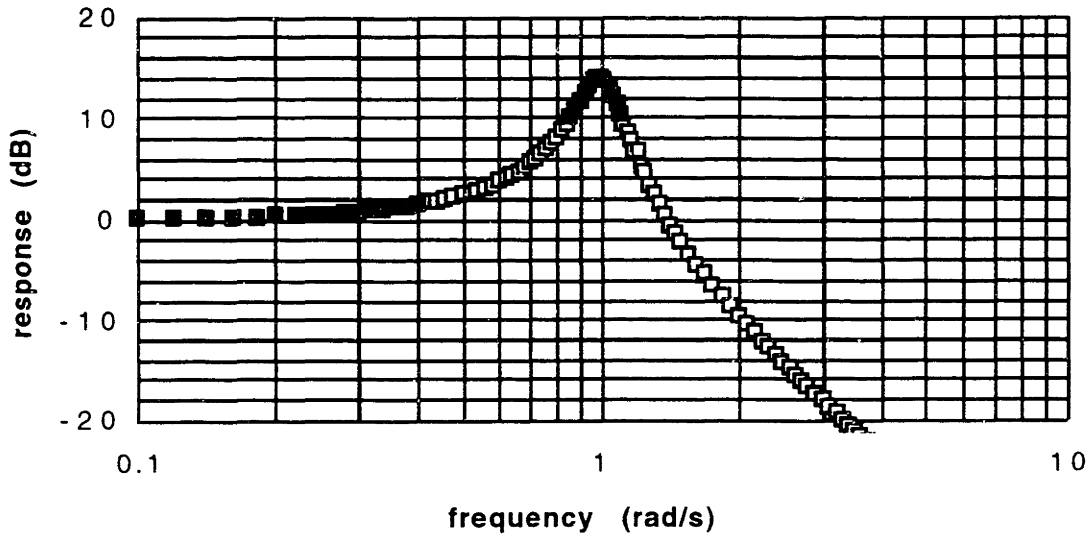

Figure 2 - Resonant Second Order System

The commercially available nozzles are designed to operate around their mechanical resonant frequency, showed as a dark range over the resonant peak in figure 2. If a nozzle could be made to operate instead in the dark region at frequencies lower than its mechanical resonance, the piezo response, and therefore the excitation to the stream, would have the same amplitude over a wide range of frequencies. This nozzle would have to transfer energy efficiently to the stream in order to get the same disturbance magnitude as commercial nozzles without the advantage of increased response at resonance.

If the amplitude of stream disturbance is no longer dependent on operating at a narrow frequency range, two immediate advantages would be gained. First, the nozzle could be used to account for a velocity ripple of about 100Hz as the printhead traverses the powder bed. Because the printhead velocity is not perfectly constant, the placement of droplets onto the powder bed is not perfectly accurate. A nozzle which had a steady breakoff excitation regardless of frequency could change its operating frequency in response to an error signal from the velocity of the printhead and place droplets in the

specified position on the powderbed without sacrificing dependable droplet formation. Second, new applications for 3D Printing are being explored in medical fields, with current emphasis on printing with viscous polymer fluids. By experimental observation, these thick fluids break off into droplets best at frequencies lower than the typical operating frequencies used for water and colloidal silica binder, and this optimum breakoff frequency is specific to each thick fluid [Serdy]. Therefore a nozzle which delivers equal excitation over a range of frequencies could be universally used for these new fluids.

2.4 - Non-wearing Nozzles

The best nozzles require little maintenance and do not need to be replaced because of wear. In this case, wear refers specifically to the enlarging of the orifice due to the constant fluid flow through them, particularly with binder that has colloidal silica. If the orifice widens, the flow characteristics will change, and the printing process will not be precise. As 3D Printing is capable of creating larger parts, the demand increases for nozzles that can jet for long periods. Currently used nickel electro-formed orifices last only about ten days before they become unusable. On the other end of the spectrum, nozzles made with alumina wire-bonding tools as nozzles exhibit no wear during the few weeks that they are in operation. Not only are wear characteristics critical for longer running parts, but recent success with replacing colloidal silica binder with a slurry of alumina particles, which wear out orifices much more quickly, increases the need for low-wearing orifices.

Chapter 3 -- Tube-piezo Nozzles

3.1 - Molded Rubber Orifice

The most successful attempt at making a nozzle which fit the design criteria discussed in chapter 2, has a rubber orifice molded around a thin sewing needle inside a 1/4in length of radially polarized tube piezo. This orifice was attached to a medical syringe to serve as the fluid delivery system. The entire assembly is shown in figure 3.

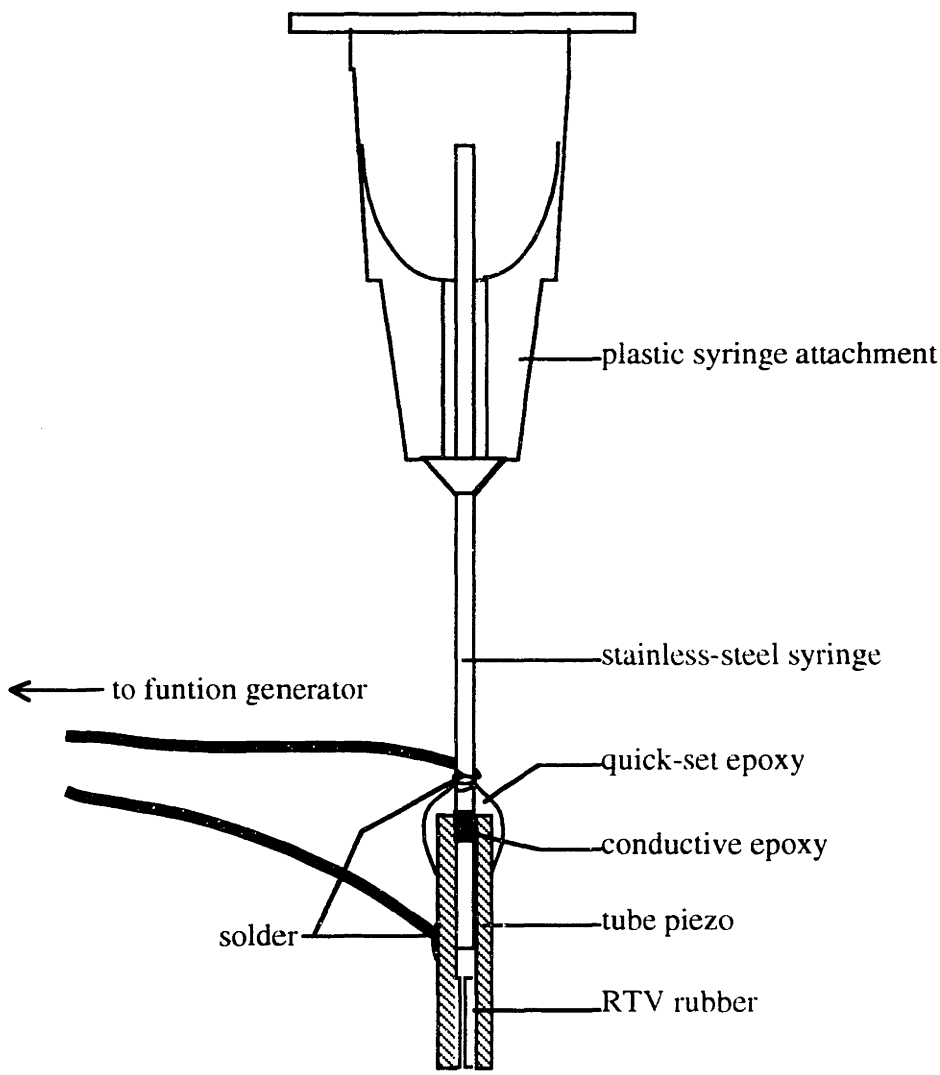

Figure 3 - Tube-piezo Nozzle

The 25mm long stainless-steel syringe is set 3.2mm deep into a 6.4mm length of Morgan Matroc PZT-5H piezo-ceramic tube. The electroded faces of the piezo are on the inner and outer cylindrical surfaces of the tube. To make the electrical connections to the piezo tube, the outer surface is soldered to the current-carrying wire, while the inner surface is electrically connected to the stainless-steel syringe with conductive epoxy and the wire is soldered to the syringe. The strong mechanical connection between the syringe and the piezo is a blob of quick setting epoxy. The entire assembly weights 0.4g. Figure 4 shows the detail in the rubber orifice and gives the dimensions of the small nozzle.

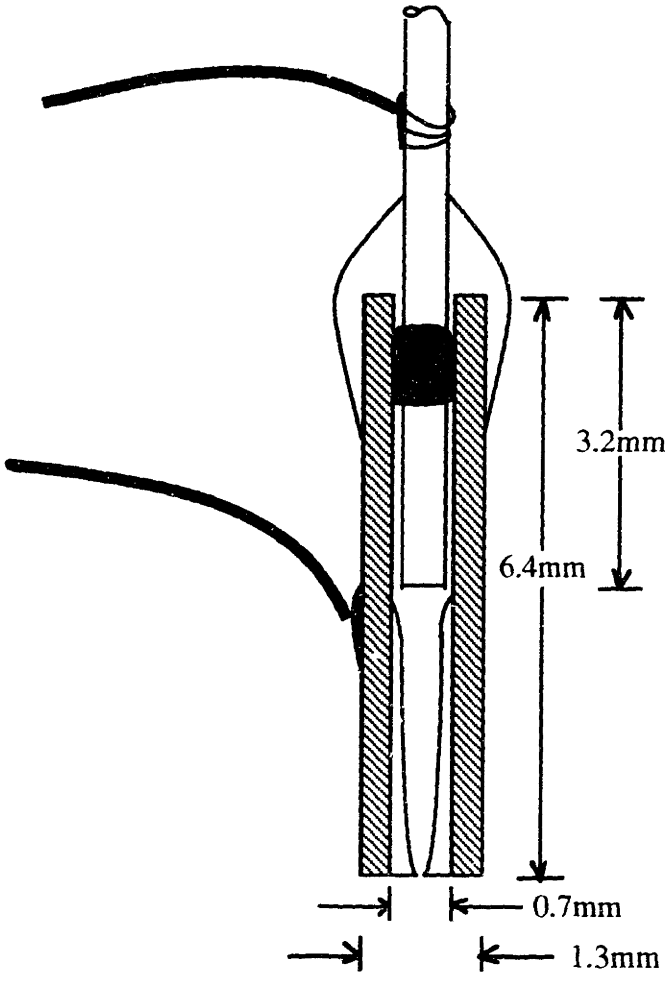

Figure 4 - Rubber Orifice Detail

A thin sewing needle proved to be both stiff and straight enough to be inserted through the syringe and be concentric with the syringe and piezo tube. The tip of the sewing needle was just smaller in diameter than the desired orifice diameter of 50μm, and so the rubber was filled in around it until just a glint of metal could be seen. After the rubber was fully cured, the sewing needle was removed leaving the orifice profile illustrated in figure 4 and an orifice diameter of approximately 50μm.

Since the orifice exit sharply defines the narrowest section of the nozzle, the expected excitation mechanism is from the radial and circumferential expansion and contraction of the piezo at the exit orifice. The piezo motion is transmitted through the rubber to "pinch" the fluid stream at the exit orifice, creating a distinct diameter change in the fluid stream, which leads to controlled droplet breakoff.

3.2 - Tube-piezo Resonance

It is desirable to have the piezo frequency resonances significantly higher than the frequency range used for droplet breakoff because higher frequencies will attenuate out, leaving the piezo driving frequency to be dominant. For the rubber orifice nozzle, the resonances of the 6.4mm length of tube piezo may be low enough to interfere with the piezo driving frequency.

To determine at which frequencies the tube piezo resonates, the tube piezo was acoustically coupled to a disc piezo with a comparable resonant frequency range. To produce acoustic coupling the disc and tube piezos were lightly clamped together, and the

disc piezo was driven with 20 volts peak-to-peak at various frequencies, while the voltage response of the tube piezo was noted. As the disc piezo is stressed electrically by the driving voltage its dimensions will change, and the tube piezo will be stressed mechanically between the disc piezo and the clamp, generating an electric charge across its electroded faces. The voltage across the electroded faces of the tube piezo will be greatest at a resonant frequency.

The resonant frequencies of the disc piezo also appear as resonant voltage across the tube piezo. In order to isolated the tube resonant frequencies, the same acoustic coupling experiment was done with two disc piezos to determine the disc piezo resonant frequencies. These disc resonant frequencies of 390kHz, 410kHz, 1050kHz, and 1100kHz were then removed from the resonant frequency spectrum of the tube piezos. The disc piezo was coupled to the tube piezo because the flat surface of the disc proved easier to clamp to the tube piezo, as opposed to clamping two tubes together. The resonant frequencies of the tube piezo are shown in figure 5.

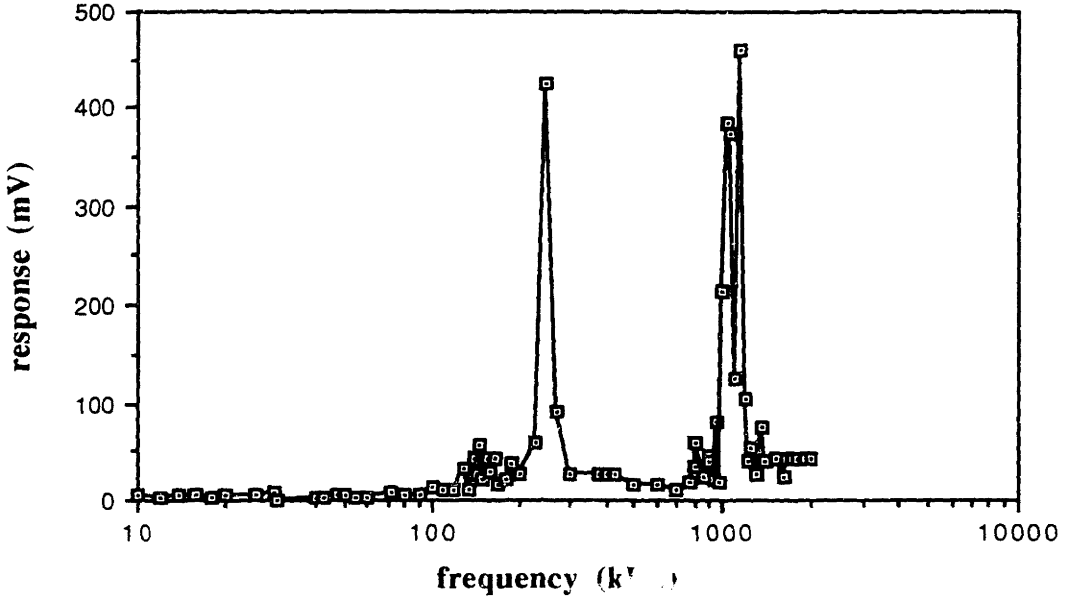

Figure 5 - Tube piezo frequencies

The resonant frequencies of the tube piezo are 250kHz, 1050kHz, and 1150kHz, which are all above the desired printing frequency range of 30-100kHz. Of these mechanical resonant frequencies, the one which may interfere the most which the driving frequency of printing is the lowest one at 250kHz. As is clear from a second-order system model of the nozzle, the highest frequencies will be the most attenuated, but a frequency of 250kHz may still have an amplitude contribution. However, this low frequency of 250kHz is for the unrestricted full 1/4in length of piezo, and when the piezo is anchored to the fluid delivery system, the resonant frequency of the attached piezo tube will be higher. The frequency will travel at the speed of sound in the material, given by [Lindeberg, 14-13]:

$$a = \sqrt{\frac{E}{\rho}} \tag{6}$$

where a is the sonic velocity, E is the elastic modulus, and ρ is the density of the material. The lowest resonant frequency is across the length of the piezo where each end of the tube is a node of vibration, so the resonant frequency is:

$$\nu = \frac{1}{2L}\sqrt{\frac{E}{\rho}} \tag{7}$$

where ν is the resonant frequency, L is the length of the piezo tube, E is the modulus of and ρ is the density of the piezo material. For the Morgan Matroc PZT-5H piezo ceramic,

E = 7.1E-10Pa, and ρ = 7,500kg/m^3, so the wave solution frequency ν = 297kHz. The experimentally determined resonant frequency of 250kHz may be different from the wave solution frequency because of the clamping restriction on the piezo. By equation 7, as the length L of the piezo decreases, its resonant frequency increases, and attaching the tube in any realistic manner to the fluid delivery system will decrease the effective resonating length and therefore increase the resonant frequency. The length of the piezo is only limited by the need to have the radial and circumferential motion uninhibited at the orifice. As a rule-of-thumb, a change in geometry three dimensions away will not affect the area in question, so for an outer piezo diameter of 1.3mm, the piezo can be attached to the fluid delivery system 3.9mm along the length and not affect the orifice motion.

Chapter 4 -- Characteristics of Rubber Orifices

4.1 - Frequency Resonance

The frequency range of the sewing needle orifice nozzle jetting with water was about 30kHz to 75kHz. Within this range droplet formation was regular and acceptable for printing. Below this range, breakoff was irregular and large irregular satellite droplets appeared. Above this range from 77kHz and higher, no breakoff occurred, in fact the stream no longer responded to any piezo driving frequency or amplitude change. More importantly, across the usable printing range, no frequency stood out as a resonant frequency, demonstrating the desired non-resonance described in chapter 2.

Figure 6 shows pictures taken from a video tape of the droplets at various frequencies with a constant 20volts peak-to-peak sinusoidal driving voltage and 1.0cc/min flow rate. Note that these pictures were taken along various parts of the stream. The second picture in the bottom row shows the droplet breakoff and two satellite drops. Every frequency in the middle range formed two satellites right after breakoff, but the satellites were the least control-impairing kind because they were small and merged with the droplet following directly behind. The first two pictures show the unusual satellites formed in the low frequency range. Droplet formation below 20kHz cannot be seen with the current set up of equipment in the lab because the LED strobe flashing in synchronization with the piezo frequency fades out below this range. The last two pictures show the cut off of droplet formation around 77kHz.

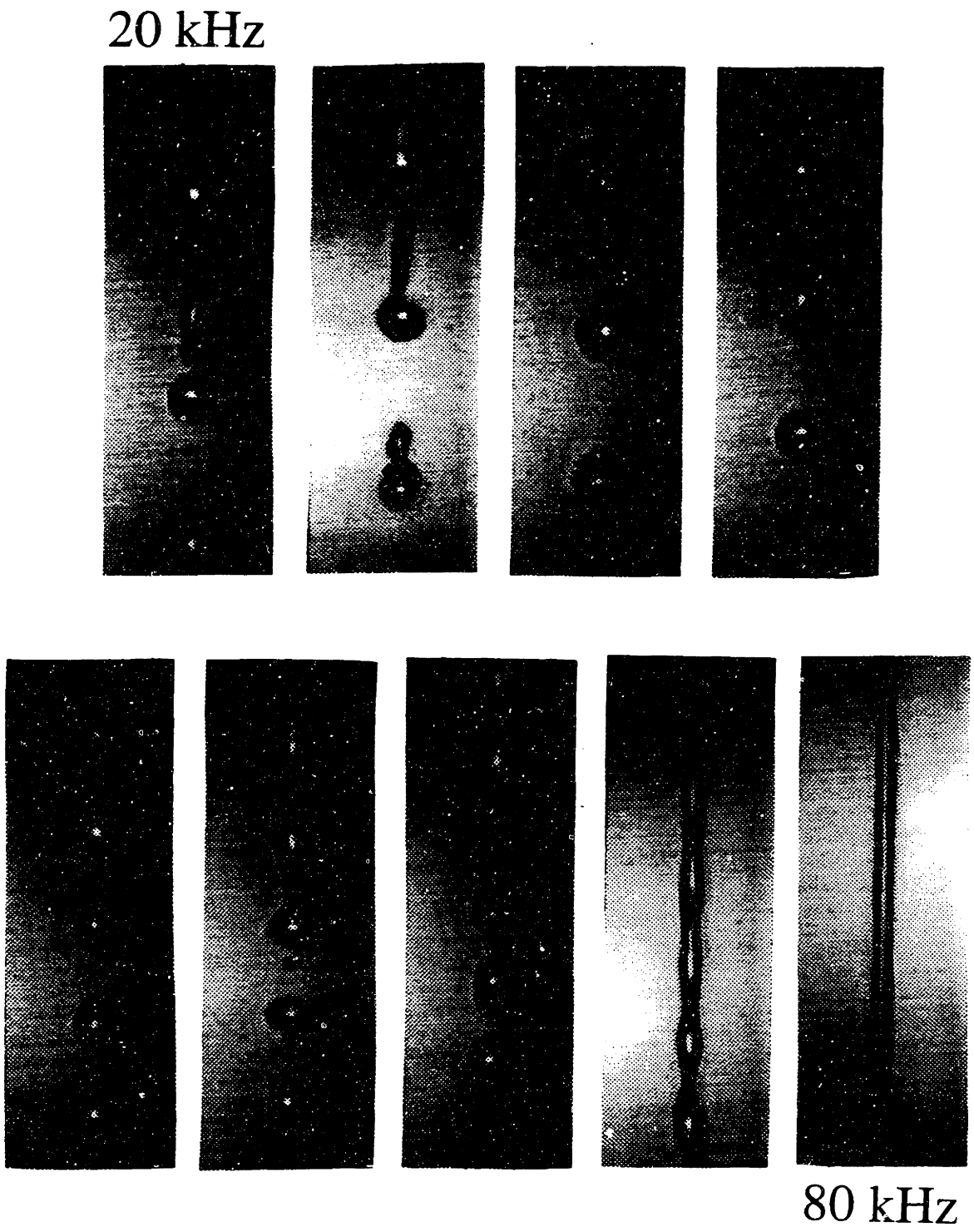

Figure 6 - Droplets at Various Frequencies

Figure 6 also shows how droplet size and the space between droplets decreases as the frequency of droplet formation increases. Droplet spacing is equal to the wavelength of breakoff, and therefore inversely proportional to the piezo frequency. By conservation of volume, the droplet diameter can be calculated as [Williams, p.53]:

$$\begin{Bmatrix}\text{Volume}\\ \text{of drop}\end{Bmatrix} = \begin{Bmatrix}\text{cross}-\text{sectional}\\ \text{area of jet}\end{Bmatrix}\begin{Bmatrix}\text{wavelength of}\\ \text{drop formation}\end{Bmatrix} \tag{8}$$

$$\left\{\frac{4}{3}\pi\frac{d_d^3}{8}\right\} = \left\{\pi\frac{d^2}{4}\right\}\{\lambda\} \tag{9}$$

where d_d is the droplet diameter, d is the jet diameter, and λ is the distance between the centers of adjacent drops measured by scrolling down the video camera and measuring the distance the video camera travels with a dial indicator. Estimating the jet diameter to be 50μm, and measuring λ = 327μm at 30kHz and λ = 163μm at 75kHz, the droplet diameter ranges from 107μm at 30kHz to 85μm at 75kHz, or 2.1x the jet diameter at 30kHz to 1.7x the jet diameter at 75kHz. This change in droplet size can affect the accuracy of 3D Printed part dimensions.

From the discussion of exponential disturbance growth in chapter 1, a resonant frequency results in a short breakoff length, so by measuring breakoff length as a function of frequency while operating at a constant voltage, resonances can be detected. Figure 7 shows the relatively smooth curve of frequency verses breakoff length without any sharp resonant frequency peaks of particularly short breakoff. Instead, there is a resonant trend where the shortest breakoff lengths occur around 60kHz. The expected frequency at the shortest breakoff length is the Rayleigh frequency, given for the inviscid case in equation 1. One uncertainty in the Rayleigh frequency calculation is the actual orifice diameter, as discussed in section 4.4. During experimental breakoff testing, the pressure driving the stream was 36psi, resulting in an orifice diameter of 44.4μm and a flow rate of 0.85cc/min.

From these values, the calculated Rayleigh frequency is 52.5kHz, in the range of short breakoff lengths seen in experiment. Another indication of resonance would be the natural frequency of the rubber. The lowest natural frequency of the rubber, in the direction of the orifice motion, will be the frequency of a wave traveling from the outer edge of the rubber (near the piezo) to the orifice, a length of 0.35mm. Using equation 7 with L = 0.35mm, E_{rubber} = 1.92MPa (see section 4.2), and ρ_{rubber} = 1.000kg/m^3, the natural frequency of the rubber is 63kHz, also in the range of short breakoff lengths as seen in experiment.

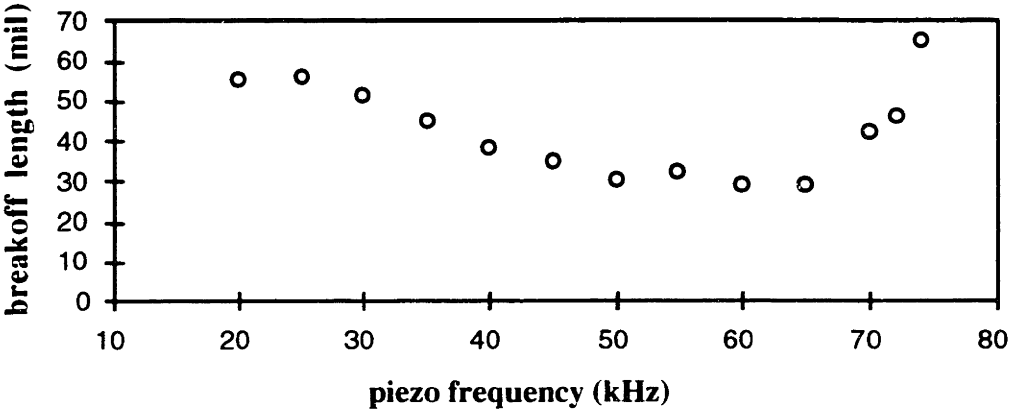

Figure 7 - Frequency Resonance

At 77kHz, the piezo-driven droplet formation ends, effectively resulting in an infinitely long breakoff length, though the stream will break up naturally at some relatively long distance from the nozzle orifice. This suggests that frequencies higher than 77kHz are attenuated by the rubber and therefore do not disturb the fluid stream. Near 20kHz, the frequency vs. breakoff length curve appears to level off. However, the LED strobe does not operate below about 20kHz, so breakoff measurement with the video camera and the dial indicator is not possible at lower frequencies.

Comparing figure 7 to an underdamped second order system reveals notable similarities. Since large amplitude response leads to short breakoff lengths, the experimental response graph in figure 7 above could be turned up-side down to fit a second order frequency/response curve like the one in figure 8 below.

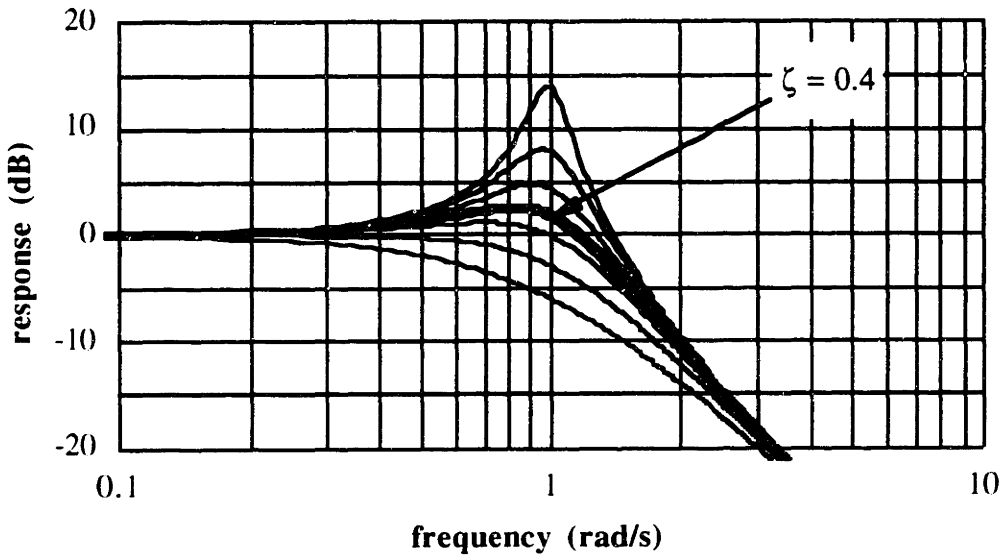

Figure 8 - Second Order Response to Frequency

The experimental curve appears to fit an underdamped resonant curve with a damping ratio of about $\zeta = 0.4$, as shown in the middle curve in figure 8. The damping ratio ζ is high due to the rubber absorbing some of the piezo response energy from the piezo motion before disturbing the stream. While this is not the frequency range below resonance as described in section 2.3, the effective small change in response amplitude over a wide range of frequencies is still achieved.

4.2 - Stiffness of the RTV Rubber

In order to effectively transfer the piezo energy through the rubber to the stream, the rubber must be relatively stiff, but still soft enough to damp the resonant frequency and provide equal response over a wide range of frequencies as discussed in section 4.1. In testing the rubber orifices, the effect of stiffness became clear. The Dow-Corning J-type rubber is fully cured after 24 hours at room temperature, but it continues to cure further for a total of four days. A simple tension test on bars of the rubber reveal that the measure of stiffness, or Modulus of Elasticity (E), is 1.69MPa after 2 days of curing, and reaches the final E = 1.92MPa after four days. The effect of this increased stiffness on breakoff length and frequency range is illustrated in figure 9, which shows breakoff length vs. piezo frequency for the same nozzle after 2 days of curing and after 7 days.

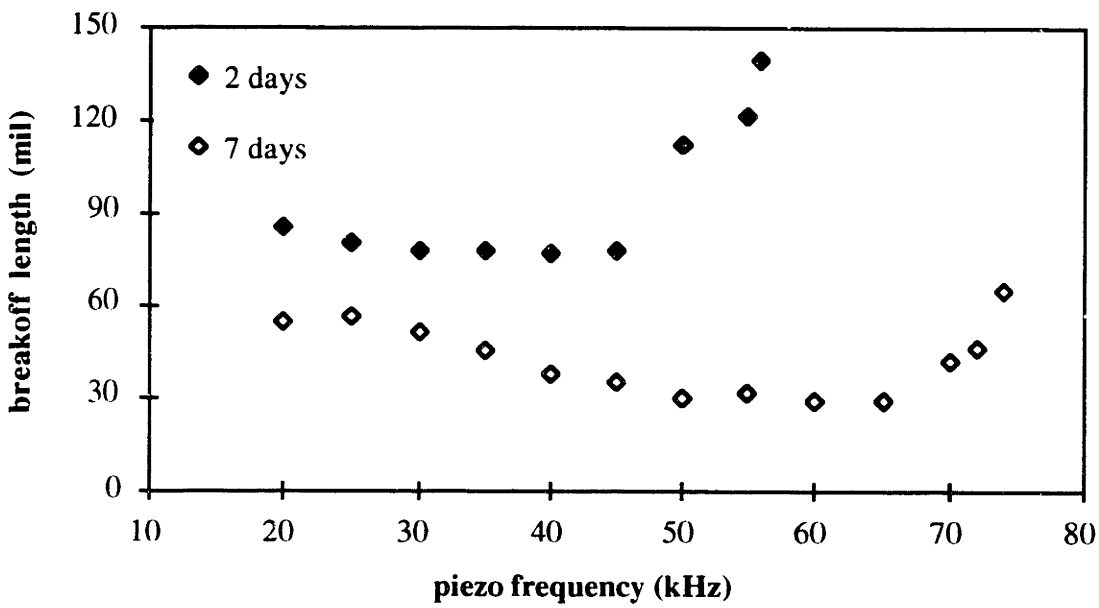

Figure 9 - Effect of Rubber Stiffness

With increased curing, and therefore increased stiffness, the breakoff length decreases. Again from equation 4,a greater disturbance of the stream results in a shorter breakoff length, which suggests that the stiffer rubber is transmitting more of the piezo motion to the fluid stream, as expected. Also, the frequency range before cut-off is increased for the stiffer rubber, suggesting that the stiffer rubber is transmitting higher frequencies which the less stiff rubber is absorbing.

This effect of rubber stiffness provides another way to design a nozzle to meet specified characteristics. And in addition to selecting an available rubber for its stiffness, temperature could be used to control or alter the stiffness of rubber. A fully cured tensile test specimen brought up to 100° C had a modulus of E = 2.88MPa, fully 50% higher than the modulus for fully cured rubber at room temperature. After cooling back down to room temperature, the bar had a modulus of E = 2.15MPa. However, the dimensions of the cooled bar were 0.8% less in all directions, so heat treatment may be problematic in designing for an accurate orifice diameter.

4.3 - Voltage Response

The amount of piezo strain is proportional to the applied electric field by a piezoelectric constant. This increased piezo motion gives increased disturbance of the stream, and from the discussion in chapter 1, the breakoff length decreases. Figure 10 shows breakoff length at various driving piezo driving voltages, and the expected decreases in breakoff length as voltage increases.

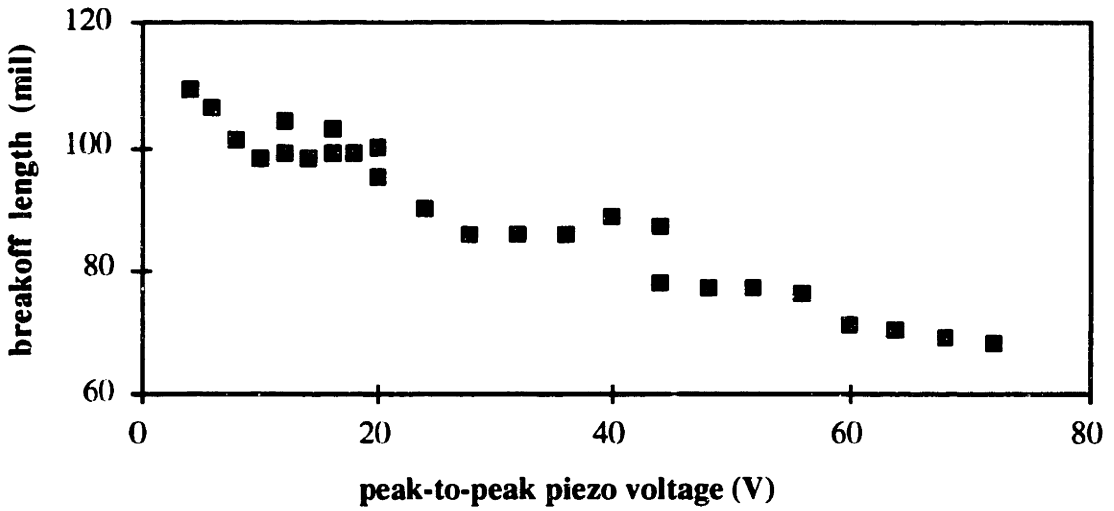

Figure 10 - Voltage response

Over this relatively small range of voltages from 2V to 72V, no dramatic resonant response at a specific voltage occurs. The noise in the data, which appears as steps as voltage increases is largely due to the distance between droplets which is roughly 10mil. If a measurement of breakoff length is taken just as a droplet is about to break off, the next measurement immediately following droplet breakoff will be about 10mil shorter due to the loss of one droplet length. Also, this test was run on a nozzle after only 2 days of curing, which accounts for the relatively long breakoff length, as discussed in section 4.2.

4.4 - Orifice Expansion

The fluid flow rate through the nozzle is controlled by holding a constant pressure of air behind it. From Bernoulli's equation for steady, incompressible, nonviscous flow without a gravity field, the mechanical energy along any streamline is constant by [Shames, p.239]:

$$\frac{v^2}{2} + \rho P = \text{constant} \qquad (10)$$

where v is the velocity of the stream, P is the stream pressure, and ρ is the fluid density. Therefore the velocity of the stream is proportional to the square root of the stream pressure. And since fluid flow rate Q is related to fluid velocity v, and orifice area A, by:

$$Q = A \cdot v \qquad (11)$$

As long as the orifice area is constant, the fluid flow rate should also increase as the square root of the pressure. But in experiment, the fluid flow rate increased much more rapidly with increasing pressure, indicating that the orifice area was increasing. The relationship of the orifice area to pressure was determined by rearranging equation 11 to solve for orifice area:

$$A = \frac{Q}{v} \qquad (12)$$

Flow rate Q can be found simply by collecting and measuring the amount of fluid to exit the nozzle in a known amount of time, and velocity v can be found by measuring the distance between droplets with the video camera and dial indicator and multiplying by the frequency of breakoff in Hertz. By assuming the orifice is circular, the orifice diameter vs. pressure can be calculated. Figure 11 shows the resulting data.

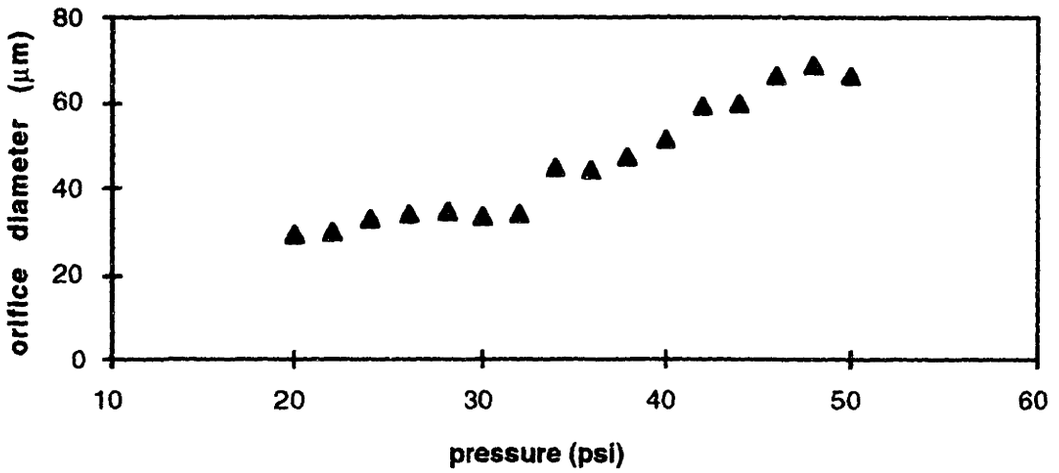

Figure 11 - Orifice Expansion

Since rubber is incompressible, the most reasonable explanation for the orifice expansion is that the rubber orifice "bows out" at the thin exit cross section, expanding with increasing fluid pressure as shown in figure 12:

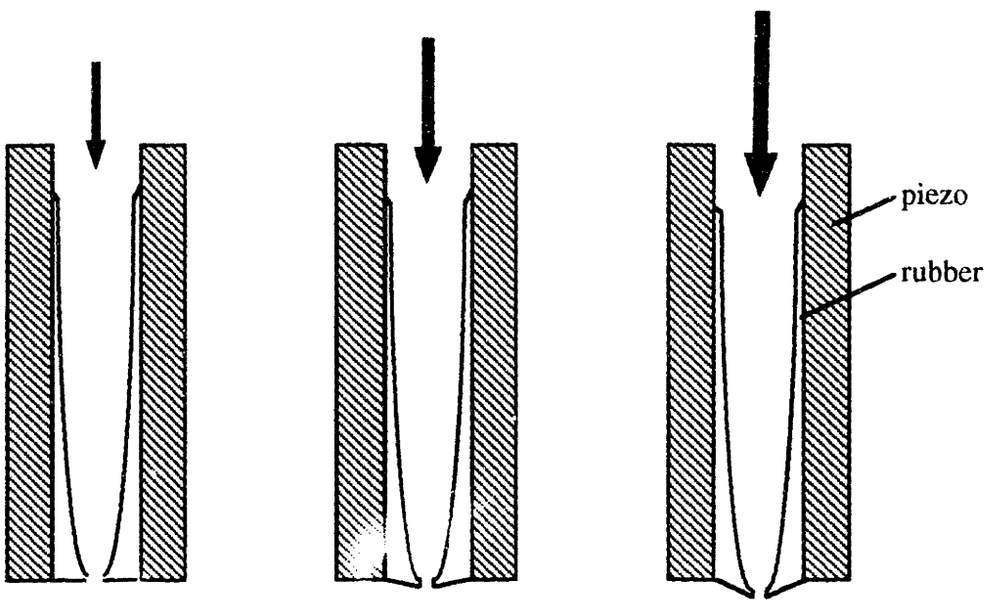

Figure 12 - Increasing Expansion of the Orifice

The characteristic of orifice expansion is undesirable because the orifice diameter is a factor in flow rate and breakoff length, and independent orifice expansion detracts from the control of those parameters. Molding the rubber into a more structurally resilient shape, as noted in section 5.2, may reduce the orifice expansion.

Chapter 5 -- Disturbance Mechanisms

5.1 - Orifice Expansion/Contraction

The simplest explanation of the breakoff excitation for the piezo/rubber orifice nozzle is that the piezo expands and contracts perpendicular to the fluid stream, and that the rubber transmits this motion to the stream by expansion and contraction of the orifice, "pinching" the fluid stream just as it exits the nozzle. This motion would be the most efficient way of directly disturbing the surface energy of the stream. To determine if this is the dominant mode of stream disturbance, a prediction of the amount of orifice displacement can be compared to the amount of disturbance necessary to cause the breakoff lengths achieved by experiment.

Rearranging equation 4 to solve for the disturbance δ_0 results in:

$$\delta_0 = \frac{d}{2}\left\{\exp\left[\frac{Z}{d\left(\sqrt{We}+3\frac{We}{Re}\right)}\right]\right\}^{-1} \qquad (13)$$

where all the values on the right side are known. Solving for δ_0 with d = 50μm, Z = 0.05in, We = 66 (water), and Re = 460, results in δ_0= 12,800Å. Therefore, if the pinching mechanism is dominant, it produces about 12,800Å of displacement to the stream. However, equation 13 may not be a good prediction of the disturbance magnitude, so the 12,800Å disturbance should be considered an order-of-magnitude approximation.

The change in orifice area is a result of both radial and circumferential piezo motion. For the piezo-ceramic material used and the size of the tube piezo, the radial and circumferential expansion and contraction mechanisms of the tube piezo nozzle have

contributions within an order of magnitude of each other, so both mechanisms must be considered. The Morgan Matroc PZT-5H piezo ceramic is designed for motion sensitivity and has particularly high piezo-electric constants in both the polarized and secondary directions. This particular piezo is polarized in the radial direction, and the piezo-electric constant perpendicular to the electrodes is d_{33} = 593E-12m/V, so the displacement across the radial thickness at 20V is 118.6Å.

The strain in the circumferential direction is a function of the electric field across the radial thickness by:

$$\varepsilon_{hoop} = d_{31} \frac{V}{t_{radial}} \tag{14}$$

where d_{31} = -274E-12m/V, V = 20V, and t_{radial} = 0.3mm. Over the circumference of the inner diameter of the piezo where I.D. = 0.67mm, the displacement in the circumference is 384.6Å.

For a peak-to-peak sinusoidal driving voltage of 40V the radial and circumferential displacements combine together in maximum expansion at +20V, and combine together in maximum contraction at -20V, changing the circular area in a cross-section of the tube piezo. This motion affects the orifice area because rubber is incompressible so the volume of the rubber cannot change with a change in shape. Assuming that the only piezo and rubber motion is perpendicular to the fluid stream, the cross-sectional area of the rubber must be constant. As the outer diameter of the rubber changes the effect on the inner diameter (which is the orifice diameter) is magnified.

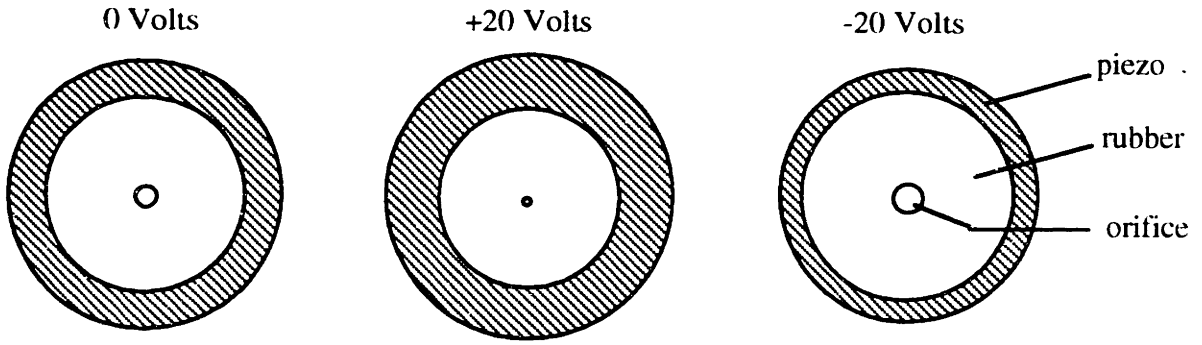

Figure 13 - Exaggerated Changes in Orifice Area with Piezo Motion

The combined effects of radial and circumferential expansion and contraction change the orifice diameter from 50μm at 0V to 49.71μm at +20V and 50.3. μm at -20V, for a total difference of about 6,100Å. Appendix B details the mathematics. The calculated disturbance of 6,100Å is just less than half of the theoretical disturbance needed to produce a breakoff length of 50mil. One source of error is from neglecting the displacement along the length of the piezo tube (the strain along the length is the same as the hoop strain in equation 14). This displacement along the length of the piezo may contribute significantly to the change in shape of the incompressible rubber, resulting in further expandsion or contraction of the orifice. Also, as stated earlier, the result from equation 13 may not reflect the actual disturbance magnitude, so 6,100Å may be all the motion required to acheive a breakoff length of 50μm.

5.2 - Other Disturbance Mechanisms

Despite uncertainty about the result of equation 13, the "pinching" of the stream at the narrowest section of the orifice may not account for all of the stream disturbance which

excites droplet breakoff. Therefore, several other mechanisms which may dominate or contribute to the droplet formation must be investigated. Among these other mechanisms are 1) A pressure wave formed in the stream by the radial motion of the piezo tube 2) A pressure wave formed in the stream by the contraction and expansion of the piezo tube along its length and 3) Vibration of the orifice exit in a direction parallel to the stream. This last mechanism is suspected of being caused by the bowing out of the rubber orifice as discussed in section 4.4, rather than the vertical motion of the entire orifice due to the expansion and contract of the tube piezo along its length, which is included as a pressure wave effect in the second disturbance mechanism.

To investigate the effects of the two pressure wave mechanisms, a nozzle which had no rubber was built and tested. Instead, the tip of a wire-bonding tool was attached to the end of the tube piezo to create a rigid orifice.

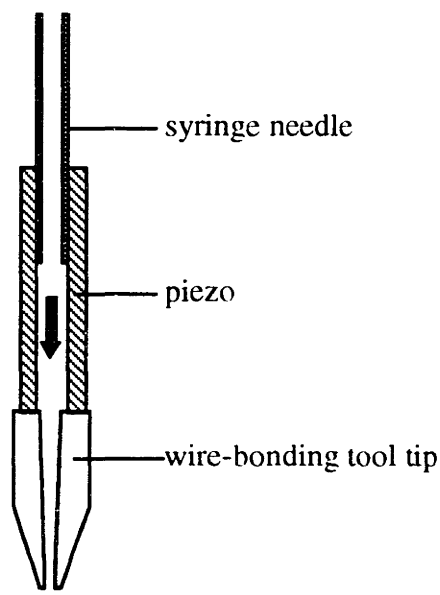

Figure 14 - Nozzle with Wire-bonding Tool Tip

This nozzle could both induce a pressure wave by the radial motion of the piezo and induce a pressure wave by the motion of the piezo along its length. However, the stream showed

no response to piezo frequency or voltage amplitude, suggesting that the tube piezo does not induce significant pressure waves, either in length or radially, which could affect droplet breakoff.

The third mechanism of excitation is more difficult to dismiss by experiment. The expansion of the rubber orifice suggests that the rubber bows outward under the pressure of the stream, but whether or not the rubber bows in and out with the piezo frequency is difficult to observe. One effort to decrease the orifice expansion and the possibility of vertical vibration at the orifice exit was to fabricate a rubber orifice in an "hourglass" shape as illustrated in figure 15. Unfortunately, attempts at molding an hourglass-shaped orifice were unsuccessful.

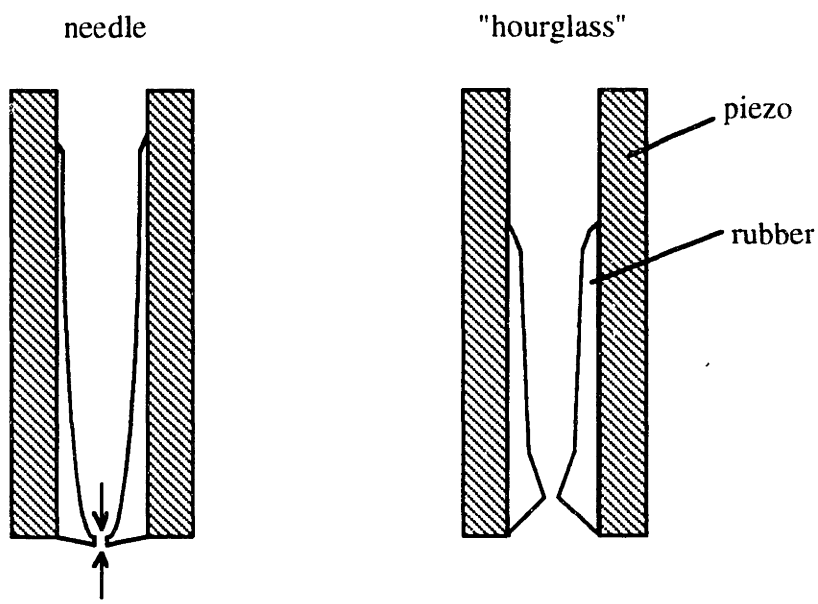

Figure 15 - Orifice Vibration

Lacking a comparable hourglass orifce, the stream disturbance from the orifice vibration is difficult judge, particularly without knowing the amount of orifice motion, if

any. Fortunately, if additional disturbance mechanisms exist, they do not hinder droplet formation.

Chapter 6 -- Future Directions

In general, the tube piezo nozzle successes proved that small, light weight, non-resonant nozzles, which may be suitable for 3D Printing, can be built. However, the basic nozzle has yet to be tested for absolute repeatability of performance. In addition, reducing or controlling the orifice expansion must be further researched, possibly with the more resilient rubber "hourglass" shape as described in section 5.2 and shown in figure 15. The rubber orifice must also be tested for wear. A first attempted test for wear under continuous binder flow was inconclusive because the fluid flow rate through the nozzle fluctuated due to fluid pressure changes in the test equipment. Finally, to ensure compatibility with 3D Printing, the nozzles must be tested for droplet generation with binder and possibly even run on the 3D Printing machine.

Furthermore, if the tube piezo nozzles are to be the next generation of nozzles used in 3D Printing, a standard manufacturing procedure should be developed. Though hopefully the nozzle design is robust enough to produce nozzles with similar operating characteristics despite current hand-fabricating techniques. Two test nozzles were made by hand, and they had similar operating characteristics such as the same usable frequency range and the same cutoff frequency to within 1Hz. A larger sample of test nozzles may reveal which operating characteristics vary the most between hand-fabricated nozzles.

And, of course, other nozzle designs should be explored. The tube piezo nozzle is only one of several designs that allows the piezo motion to directly affect the fluid stream. Other ideas may center on multiple-jet applications. In particular, an idea that may form the rubber orifice nozzles directly into a multiple-jet nozzle involves using a piezo strip with drilled holes in a line across its length. These holes would act like the inner diameter of the piezo tube, and rubber orifices formed with the sewing needle and medical syringes would be molded into these holes. The expansion and contraction of the piezo strip across both its

length and width would change the area of the holes, and the rubber would transmit the disturbance to the fluid stream [Serdy]. Figure 16 shows a schematic drawing of the multiple-jet idea.

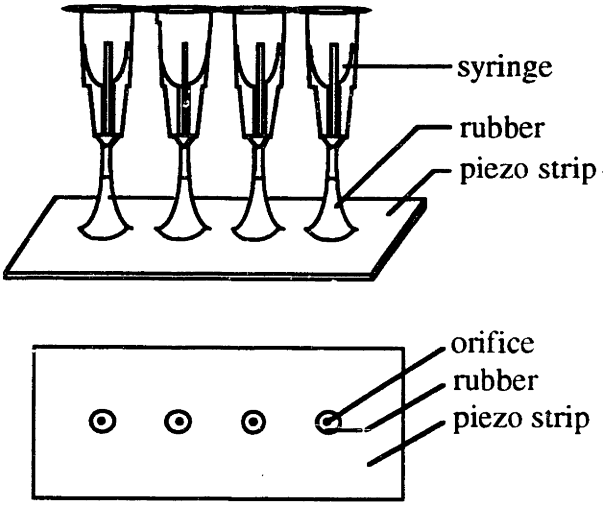

Figure 16 - Piezo Strip Multiple-jet Nozzle

Other initial ideas include breakoff disturbance from the torsional motion of a square orifice, and rapid side-to-side motion of the orifice to excite breakoff.

Appendix A -- Nozzle Data for Breakoff Length and Orifice Diameter

pressure (psi)	flow rate (cc/min)	distance between 5 drops (mil)	Peak-to-peak voltage (V)	frequency (kHz)	breakoff length (mil)
20	0.35	41.5	20	40	26
22	0.3	35	20	40	28
24	0.375	36	20	40	29
26	0.4	35	20	40	26
28	0.375	32	20	40	36
30	0.4	37	20	40	36
32	0.4	35	20	40	38
34	0.8	41	20	40	47
36	0.85	45	20	40	46
38	0.95	44	20	40	62
40	1.25	49	20	40	73
42	1.7	50	20	40	114
44	1.8	52	20	40	90
46	2.4	57	20	40	123
48	2.6	57	20	40	114
50	2.4	57	20	40	124

pressure (psi)	jet velocity (m/s)	orifice area (m^2)	orifice diameter (μm)	Rayleigh frequency (kHz)
20	8.43	6.92E-10	29.68	63.00
22	7.11	7.03E-10	29.92	52.71
24	7.32	8.54E-10	32.98	49.18
26	7.11	9.37E-10	34.55	45.65
28	6.50	9.61E-10	34.98	41.21
30	7.52	8.87E-10	33.60	49.61
32	7.11	9.37E-10	34.55	45.65
34	8.33	1.60E-09	45.14	40.92
36	9.14	1.55E-09	44.41	45.65
38	8.94	1.77E-09	47.49	41.75
40	9.96	2.09E-09	51.62	42.77
42	10.16	2.79E-09	59.59	37.81
44	10.57	2.84E-09	60.13	38.97
46	11.58	3.45E-09	66.31	38.73
48	11.58	3.74E-09	69.02	37.21
50	11.58	3.45E-09	66.31	38.73

Appendix B -- Calculation of Orifice Motion

In order to calculate the maximum change in the orifice diameter, the maximum change in the inner diameter of the piezo tube must be calculated first. The tube piezo changes as a result of both radial and circumferential motions. Looking first at the 118.6Å expansion of the radius of the tube, the expansion is equal away from a neutral circumference that stays the same length.

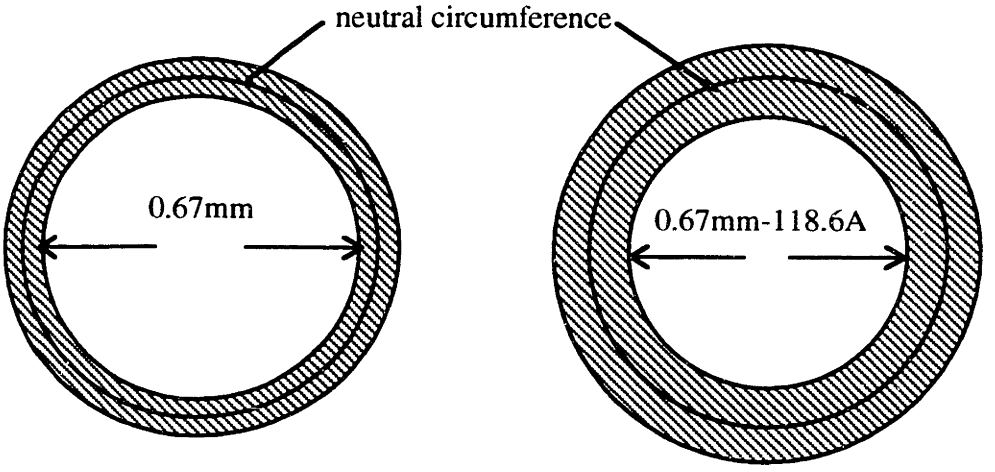

Figure 17 - Radial Piezo Expansion

This radial expansion reduces the inner diameter of the tube from 0.67mm to a total of (0.67mm - 118.6Å).

When the radius expands, the circumference contracts since the piezo-electric constant d_{31} is negative. The circumferential contraction removes 557Å from the total circumference of the original neutral circumference.

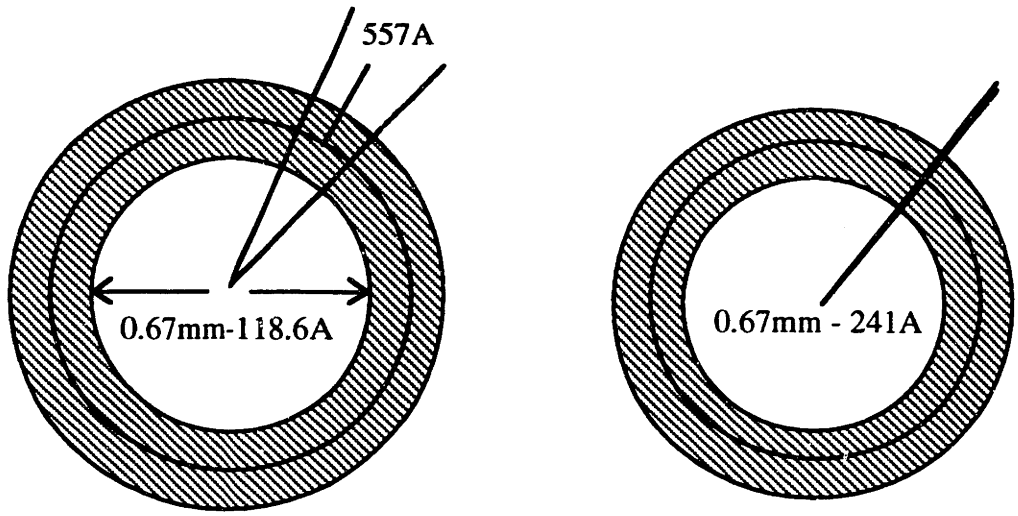

Figure 18 - Circumferential Piezo Contraction

From the constant angle of contraction θ and the neutral circumference diameter of 0.97mm, the total circumferential contraction on the radially contracted inner diameter can be calculated as:

$$\frac{\theta}{360^{\circ}} = \frac{557\text{Å}}{\pi \cdot 0.97\text{mm}} = \frac{x}{\pi \cdot (0.67\text{mm} - 118.6\text{Å})} \qquad (14)$$

where x is the circumferential contraction on the inner diameter. In this case, x = 385Å. Therefore, the final inner diameter, calculated from the change in circumference, is:

$$I.D. = \frac{\pi\left(0.67\text{mm} - 118.6\text{Å}\right) - 385\text{Å}}{\pi} \qquad (15)$$

for a total difference from the original inner diameter of 241Å. In a similar calculation of the inner diameter when the radius is contracted and the neutral circumference is expanded, the difference from the original diameter is slightly less, but also rounds to 241Å.

This change in inner diameter of the piezo relates to the diameter of the orifice because rubber is incompressible, and therefore the area of the rubber must remain the same. The original area of the rubber at 0 Volts on the piezo is the area inside the piezo of inner diameter 0.67mm minus the area of the orifice of diameter 50μm, or:

$$A_{rubber} = \pi\left(\frac{0.67mm}{2}\right)^2 - \pi\left(\frac{50\mu m}{2}\right)^2 \qquad (16)$$

Since A_{rubber} is a constant, as the value currently at 0.67mm changes, the orifice diameter currently at 50μm must change. The orifice diameter changes from 49.7094μm at +20V to 50.3220μm at -20V for a total difference of 6.126Ä.

References

Lindeberg, Michael R., *Engineer-in-Training Reference Manual.* Belmont, CA: Professional Publications, Inc. 1992.

Serdy, James. MIT 3D Printing Staff. Conversations with, Mar - Apr 1994.

Shames, Irving H., *Mechanics of Fluids, 3rd. Ed.* New York: McGraw-Hill, Inc., 1992.

Williams, Paul. "Three Dimensional Printing: A New Process to Fabricate Prototypes Directly from CAD Models." MIT, Master's Thesis, 1990.

THESIS PROCESSING SLIP

FIXED FIELD: ill. _____ name _____

index _____ biblio _____

▶COPIES: (Archives) Aero Dewey Eng Hum
Lindgren Music Rotch Science

TITLE VARIES: ▶☐ _____

NAME VARIES: ▶☐ _____

IMPRINT: (COPYRIGHT) _____

▶COLLATION: 53p.

▶ADD. DEGREE: _____ ▶DEPT.: _____

SUPERVISORS: _____

NOTES:

cat'r: date:

page: J33

▶DEPT: M.E.

▶YEAR: 1994 ▶DEGREE: B.S.

▶NAME: HAMEENANTTILA, TIINA